ANODIC AND CATHODIC PROCESSES IN PIPERIDINIUM-BASED IONIC LIQUID MIXTURES WITH $AlCl_3$

Mandar S. Risbud[a],[b], Ring Kononov[a], Martin Bucknall[c], Barry J. Welch[a], John F. McCann[a], and Maria Skyllas-Kazacos[a]*

Keywords: aluminium chloride, cyclic voltammetry, ionic liquids, Al electro-deposition.

Low temperature molten salts based on ionic liquids have received considerable attention over the last 3 decades as potential alternative solvents for aluminium reduction. Recent reports in the literature have identified 1-propyl-1-methylpiperidinium bis(trifluoromethylsulfonyl) amide ($[C_3mpip][NTf_2]$) as a promising candidate for low temperature aluminium reduction processes. The formation of aluminium metal deposition was confirmed in these studies by both visual inspection and SEM-EDX analysis in the selected mixtures with $AlCl_3$, but little is known about the anodic processes occurring in the cell. This work presents the results of a preliminary electrochemical study of the anodic and cathodic reactions occurring in the ionic liquid mixtures 1-propyl-1-methylpiperidinium bis(trifluoromethylsulfonyl)amide ($[C_3mpip][NTf_2]$) with $AlCl_3$ at different temperatures, concentrations and electrode materials. Analysis of voltammetric responses of $[C_3mpip][NTf_2]$-$[AlCl_3]_x$ for x=0.3 indicated that the anodic process is limited by mass transport for this particular electrolyte composition. In addition, the formation of Cl_2 was confirmed to take place at a dimensionally stable anode. Aluminium deposition experiments gave inconsistent results however and gas analysis indicated that the $[C_3mpip][NTf_2]$-$[AlCl_3]_x$ mixture at a prolonged elevated temperature at least partially decomposes into fluoro-carbons and chloro-compounds.

* Corresponding Author
Phone: +61 2 9385 4335
Fax: +61 2 9385 5966
E-Mail: m.kazacos@unsw.edu.au
[a] School of Chemical Engineering and Industrial Chemistry, University of New South Wales, Sydney, NSW 2052, Australia;
[b] Present address: Corrosion Centre for Education, Research and Technology, School of Chemical and Petroleum Engineering, Curtin University, Technology Park, GPO Box U1987, Perth, WA 6845, Australia;
[c] Bioanalytical Mass Spectrometry Facility, University of New South Wales, Sydney, NSW 2052, Australia.

1. Introduction

Aluminium is the most abundant element found in nature and has wide range of applications in automotive, aviation, ships and food packaging industries. Its corrosion resistance and light weight makes it one of the most widely used metals around the world. However due to its reactivity it does not occur in the free elemental state in nature and has to be extracted from bauxite using a very high energy intensive process. The electro-deposition of aluminium from aqueous solution is not feasible as the reduction of water to hydrogen occurs before the negative potential required for the reduction of aluminium ions can be reached. Therefore the potential electrolytes used for aluminium deposition are molten salts or non-aqueous organic solvents. The conventional Hall-Heroult process originally developed in 1886[1] is still the primary process used for aluminium production worldwide. This involves electrolysis at a very high temperature (950-1000 °C), of calcined alumina obtained from refined bauxite from the Bayer process. This process has very high energy consumption, complicated operation and also produces emissions of gaseous hydrofluoric acid (HF) and other vapourised fluorides formed by hydrolysis during the electro-winning process. A further drawback of the Hall-Heroult process is the use of a consumable anode that gives rise to the formation of CO_2 as a by-product of the electrowinning process[2]. Incremental improvements to the Hall-Heroult process have occurred over the last decade, especially in the area of process control where major reductions have been made in anode effects and accompanying CFC emissions. Despite these improvements, however, no major breakthroughs which would ameliorate the main disadvantages of the current Hall-Heroult process are likely to occur[3]. In recent years with growing awareness about global warming, cleaner and greener alternatives are being sought to make the process more environment friendly. Over the last few decades the development of ionic liquids has provided an alternative approach for a cleaner and less energy-intensive process for low temperature aluminium electro-deposition.

Ionic liquids generally have melting points below 100 °C, with high conductivity, high solubility of metal salts and a wide electrochemical window that allows the reduction of highly electro-active ions, making them an attractive alternative to high temperature molten salts with additional benefits such as low operational cost, low energy consumption[4-7]. Aluminium electro-deposition from aromatic hydrocarbons and ether has had limited success due to factors such as low electrical conductivity, narrow electrochemical windows and the pyrophoric nature of the materials involved[8,9]. Extensive work has been done for aluminium electro-deposition using chloroaluminate ionic liquids showing successful electro-deposition[4,9-29]. These studies indicate that the aluminium electro-deposition occurs only from Lewis acid melts where the molar ratio of

$AlCl_3$/IL is greater than 1. At lower molar ratios (Lewis base), the prominent aluminium species in the electrolyte is $AlCl_4^-$ and in this case the organic cations undergo reduction at lower negative potentials than the dominant $AlCl_4^-$ anion[30].

In the case of Lewis acid melts, the $AlCl_4^-$ forms a further complex with $AlCl_3$ leading to formation of the $Al_2Cl_7^-$ ion which is the electro-active species responsible for Al electro-deposition. The reaction can be represented as follows[30,31].

$$4Al_2Cl_7^- + 3e^- \rightarrow Al + 7AlCl_4^- \quad (1)$$

Despite success in laboratory studies, aluminium electro-deposition using chloroaluminate ionic liquids has thus far been not commercially attractive due to their moisture sensitivity and air instability. Recent reports in the literature have identified 1-propyl-1-methylpiperidinium bis(trifluoro-methylsulfonyl) amide ($[C_3mpip][NTf_2]$) as a promising candidate for low temperature aluminium reduction processes[25-28,32]; however, little is known about the electrochemical reactions occurring in the cell. In the present work, we have conducted a preliminary investigation of the anodic reaction taking place in $[C_3mpip][NTf_2]$-$[AlCl_3]_x$ mixtures using glassy carbon electrodes and dimensionally stable anodes (DSA) (Ir_2O_3 on Ti) at various compositions and temperatures. The cathodic reactions have also been the subject of a preliminary investigation at a range of temperatures, as has the stability of the ionic liquid under anticipated likely operating conditions for metal deposition.

2. Experimental section

2.1. Synthesis of ionic liquid

N-Methylpiperidine (99 wt%), 1-iodopropane (99 wt%), acetonitrile (99.8 wt%) and acetone (99.9 wt%) were used as received from Aldrich.

Bis(trifluoromethane)sulfonimide lithium salt ($LiNTf_2$) (99.95 wt%) was purchased from Iolitec (Germany). The white hygroscopic powder was kept in a glove box with moisture and oxygen levels ~ 5 ppm. Milli-Q deionized water was used for the final liquid product rinsing. The theoretical yield of $[C_3mpip][NTf_2]$ for the first batch was 75 ml (108.8 g) whereas the theoretical yield for the second and third batches was 250 ml (362.5 g), assuming a $[C_3mpip][NTf_2]$ density of 1.45 g/ml.

The C_3mpip-I solid precursor was synthesized by mixing N-Methylpiperidine and 1-iodopropane for 24 hours in a nitrogen atmosphere resulting in the following reaction:

Mpip (liquid) + 1-iodopropane (liquid) → C_3mpip-I (solid)

The reaction was performed with 5 wt% excess of 1-iodopropane with addition some acetone. An ice bath was used in the first 3-4 hours to prevent the overheating of the mixture (although no significant heat effects were observed). The resultant yellow solid agglomerate was crushed into powder and repeatedly washed with acetone and collected with a Buchner funnel. The white powder was collected and dried under vacuum at room temperature for at least 48 h. The dried solid was recrystallised using acetonitrile. The C_3mpip-I saturation concentration level was approximately 36 g/100 ml of acetonitrile at temperature close to boiling temperature of 82 °C. The hot saturated solution was either left on the bench top to cool down to room temperature for 1-2 h or placed in a freezer overnight. The crystalline product was collected and washed with cold acetonitrile on the Buchner funnel. The use of a freezer in the batch-3 recrystallisation was an attempt to achieve better final yield. The white crystalline product from each batch was dried in a desiccator under vacuum for at least 48 h. In all drying and mixing steps described above aluminium foil was used to cover flasks and desiccators to minimise the C_3mpip-I exposure to light and prevent oxidation of iodide (I^-) to iodine (I_2).

The ionic liquid $[C_3mpip][NTf_2]$ was synthesised via an ion exchange reaction between the C_3mpip-I precursor and bis(trifluoromethane)sulfonimide lithium salt:

C_3mpip-I (aqueous) + $LiNTf_2$ → $[C_3mpip][NTf_2]$ (liquid) + LiI (aqueous)

Table 1. Phase behavior of $[C_3mpip][NTf_2]$-$[AlCl_3]_x$ sample mixtures at different IL:$AlCl_3$ molar ratios and temperatures

x ($AlCl_3$)	**0.30**	**0.50**	**0.70**
22 °C	yellowish white solid paste	grey-brownish gel-like solid	brownish gel-like solid
50 °C	clear, light yellowish monophasic solution	grey-brownish gel-like solid	brownish gel-like solid
60 °C	monophasic yellowish solution	biphasic layers (almost equal quantity), upper layer brownish, lower turbid white	brownish gel-like solid
70 °C	monophasic yellowish solution	biphasic layers (almost equal quantity), upper layer brownish, lower turbid white	biphasic layers (lower layer ~ 33 % of total volume). Upper layer dark brown colour, lower layer is clear colourless solution.
80 °C	monophasic yellowish solution	biphasic layers (almost equal quantity), upper layer brownish, lower turbid white	biphasic layers (lower layer ~ 33 % of total volume). Upper layer dark brown colour, lower layer is clear colourless solution.
90 °C	monophasic yellowish solution	biphasic layers (almost equal quantity), upper layer brownish, lower turbid white	biphasic layers (lower layer ~ 33 % of total volume). Upper layer dark brown colour, lower layer is clear colourless solution.

Equimolar amounts of $[C_3mpip][NTf_2]$ and $LiNTf_2$ were dissolved in Milli-Q water and then mixed together. The resultant biphasic mixture which had a slightly brown or yellow colour was stirred for 24 h under a nitrogen atmosphere. The lower phase of the biphasic mixture containing the crude $[C_3mpip][NTf_2]$ product was repeatedly washed with Milli-Q water using a separating funnel. Batches 1 and 2 were each rinsed 10 times although 6-7 times was enough to get rid of colouration and achieve a negative iodide test by $AgNO_3$. Batch 3 was washed 20 times and a negative silver test was confirmed after 8 times rinsing. The final ionic liquid product retained a very faint yellow tone. The residual water was removed in vacuo on a rotary evaporator. The products were stored in a flask inside a desiccator. We chose not to take any additional precautions in terms of lowering moisture content of the ionic liquid, since we wanted to evaluate the commercial viability of these ionic liquids for aluminium deposition when the moisture content in the liquids was at the upper end of the spectrum.

2.2. IL-$AlCl_3$ mixtures preparations

$AlCl_3$ (99.99%, Sigma) was dissolved slowly in $[C_3mpip][NTf_2]$ with stirring at room temperature in a glove box under nitrogen atmosphere and heated to complete dissolution. Table 1 shows the phase behavior of these mixtures at various temperatures and compositions.

2.3. Electrochemical cell and instrumentation

A three-electrode cell consisting of a Pyrex glass cylindrical vessel with a flat-flange joint at the top was used for cyclic voltammetry tests of $[C_3mpip][NTf_2]$-$[AlCl_3]_x$ mixtures. The Pyrex top, which was connected to the cell, had another glass flange joint with three standard glass sockets for the working, counter and reference electrodes. The electrochemical cell assembly was carried out in a nitrogen atmosphere environment of a glove box with oxygen and moisture level less than 5 ppm. After filling the cell with electrolyte components and inserting the electrodes into the sockets, the air-tight cell assembly was removed from the glove box to carry out the electrochemical studies.

A computer programmable Solartron SI 1287 potentiostat was used to study the electrochemical behavior of $[C_3mpip][NTf_2]$-$[AlCl_3]_x$ mixtures. The working electrodes were a Metrohm Teflon sheathed glassy carbon (D= 2 mm), and a dimensionally stable anode (DSA) (Ir_2O_3 on Ti). The glassy carbon electrodes were polished to a mirror-like finish, sonicated, washed with acetone and dried in an oven at 60 °C for 3-5 hours prior to the cyclic voltammetry tests. The glassy carbon rod had a diameter of 2 mm while the dimensionally stable anode was a 1 cm wide plate that was dipped into the melt to a fixed immersion depth. The counter electrode used for all the experiments was a graphite rod and the reference electrode consisted of silver wire dipped into a solution of silver triflate in the ionic liquid under investigation[26].

3. Results and discussion

3.1. Electrochemical study

Cyclic voltammetry was used to investigate both the cathodic and anodic processes in pure $[C_3mpip][NTf_2]$ and $[C_3mpip][NTf_2]$-$[AlCl_3]_x$ mixtures. Figure 1 depicts the voltammetric responses obtained for a glassy carbon working electrode in pure $[C_3mpip][NTf_2]$ at various temperatures (60, 70, 80, 90 °C) at a scanning rate of 100 mV s^{-1}. A representative voltammetric response from Figure 1 for pure $[C_3mpip][NTf_2]$ at glassy carbon electrode at 80 °C, 100 mV s^{-1} is depicted in Figure 2.

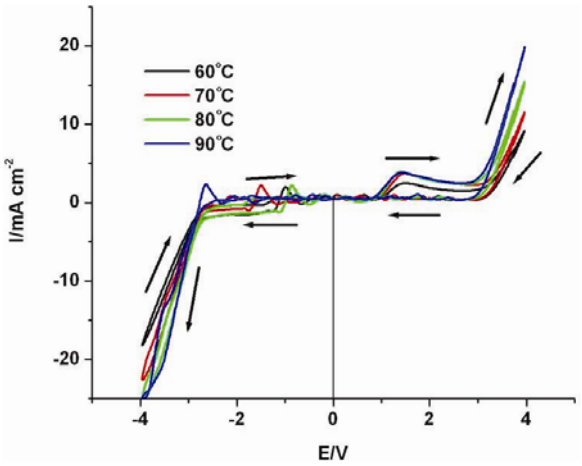

Figure 1. Voltammetric responses for glassy carbon working electrode in pure $[C_3mpip][NTf_2]$ at various temperatures (60, 70, 80, 90 °C), 100 mV s^{-1}.

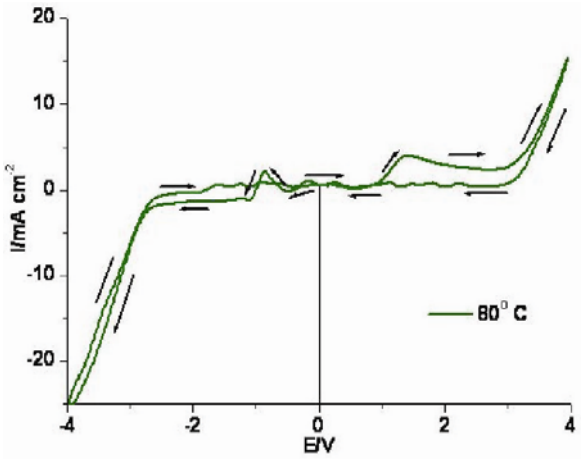

Figure 2. Representative voltammetric response from Figure 1 for pure $[C_3mpip][NTf_2]$ at glassy carbon electrode at 80 °C, 100 mV s^{-1}.

During cyclic voltammetry, the potential was swept from 0 V vs the reference electrode to –4V, then to +4V and then back to 0 V. The wide scanning range as opposed to the much narrower scanning range of about 1.8 to –1.1V (vs $Fc|Fc^+$) reported by earlier workers[26] was chosen so as to provide an indication of what was occurring over a broader voltage range. As seen from the

Figure 1, the decomposition of the pure ionic liquid would appear to start at around –2.8 V and +3 V on the cathodic and anodic sides respectively. Figure 3 depicts the voltammetric response for $[C_3mpip][NTf_2]$-$[AlCl_3]_x$ mixtures at 80 °C at various $AlCl_3$ mole fractions (x = 0.3, 0.5, 0.7).

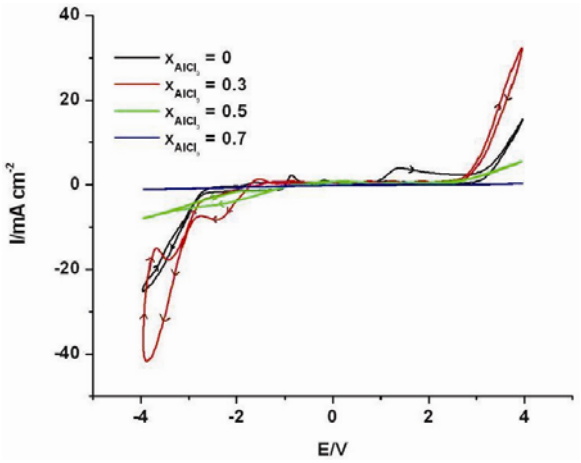

Figure 3. Voltammetric response for glassy carbon working electrode in pure $[C_3mpip][NTf_2]$-$[AlCl_3]_x$ mixtures with increasing $AlCl_3$ (x = 0, 0.3, 0.5, 0.7) at 80 °C, 100 mV s^{-1}.

A cathodic reduction wave which is apparently due to the reduction of an aluminium species in the ionic liquid electrolyte (given that it is not present when Al is not present in the electrolyte – see Figure 1) starts in the x = 0.3 mixture at around –1.7 V (see Figure 3). Figures 4 and 5 depict the voltammetric response for a $[C_3mpip][NTf_2]$-$[AlCl_3]_x$ mixture (x = 0.3) at various temperatures (50, 60, 70, 80 and 90 °C) from –4 V to +4 V. Figure 6 shows the cyclic voltammetric responses at various scan rates for x=0.3 at 50 °C.

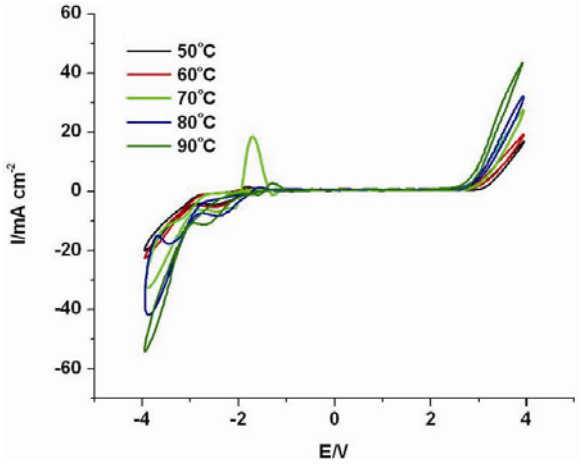

Figure 4. Voltammetric response for glassy carbon working electrode in a $[C_3mpip][NTf_2]$-$[AlCl_3]_x$ mixture (x = 0.3) at various temperatures (50, 60, 70, 80 and 90 °C), 100 mV s^{-1}.

As per Figure 3 in Figure 4 the cathodic reduction wave which is apparently due to the reduction of an aluminium species in the ionic liquid electrolyte (given that it is not present when Al is not present in the electrolyte – see Figure 1) generally starts in the x = 0.3 mixture at around –1.7 V apparently regardless of the temperature of the electrolyte although unlike Figure 3 the onset of the cathodic wave is masked somewhat by a large anodic peak that appears in the cyclic voltammogram scan at 70 °C as shown in Figures 4 and 5.

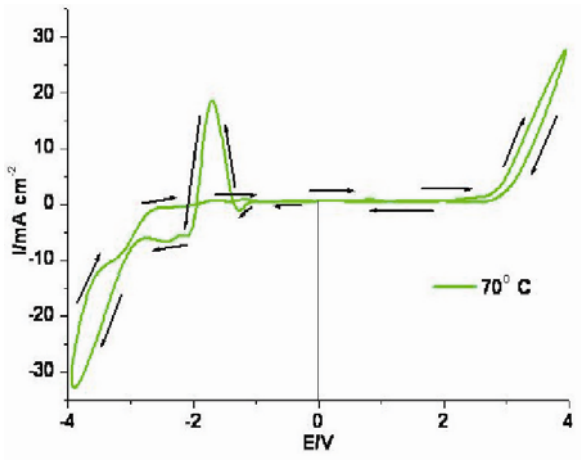

Figure 5. Representative voltammetric response from figure 4 for $[C_3mpip][NTf_2]$-$[AlCl_3]_x$ mixture (x = 0.3) at glassy carbon electrode at 70 °C, 100 mV s^{-1}.

As can be seen from Figs. 3 and 4 the aluminium cathodic reduction peak seems to be present for x=0.3 at temperatures 50-90 °C whereas according to the literature temperatures greater than 80 °C were required to achieve Al deposition[26]. Surprisingly, however, the voltammetric results presented in Figure 3 indicate that increasing the $AlCl_3$ molar ratio does not produce an increase in the reduction peak height as would be expected if the concentration of the electro-active aluminium species had increased. This suggests a complex equilibrium associated with the formation of the electro-active species produced as a result of a reaction between $[NTf_2]^-$ and $AlCl_3$. Earlier workers have attributed this electro-active species to be $[AlCl_3(NTf_2)]^-$[26].

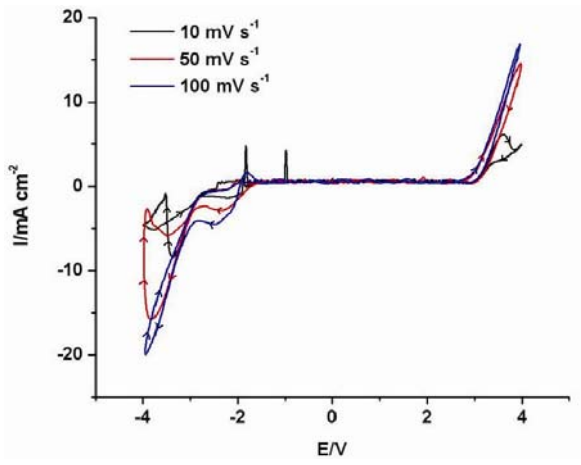

Figure 6. Voltammetric response for glassy carbon working electrode in a $[C_3mpip][NTf_2]$-$[AlCl_3]_x$ mixture (x = 0.3) at various scan rates (100, 50, 10 mV/s), 50 °C.

A positive current peak is seen in each of the voltammograms of Figures 1 to 6 for scans in the cathodic direction of a glassy carbon working electrode in the voltage range –0.5 to –3 V vs Ag triflate electrode. The magnitudes and positions of the positive current peaks at different temperatures were inconsistent with one another as is especially apparent in the voltammograms of Figures 4, 5 and 6 which utilized a $[C_3mpip][NTf_2]$-$[AlCl_3]_x$ (x=0.3) mixture. The magnitude of the positive current peak appearing at about –1.75 V vs Ag triflate in the cathodic scan at 70 °C is much greater than the positive current peaks occurring in the same regions of the scans at 50 °C, 60 °C, 80 °C and 90 °C. Whilst it is not clear as to what caused this variation it is noted that the anodic peaks of variable magnitude and position which appear to be at least partially temperature dependent are clearly present in the region of about –0.9 to –2.8 V vs Ag triflate in voltammetric scans of pure $[C_3mpip][NTf_2]$ when scanning in the cathodic direction (see *e.g.* Figure 1) and in the region of about –0.9 to –2.9 V vs Ag triflate in voltammetric scans of $[C_3mpip][NTf_2]$-$[AlCl_3]_x$ mixtures when scanning in the cathodic direction (see e.g. Figures 3 to 6). It is noted from the observations described in Table 1 that the appearance of a $[C_3mpip][NTf_2]$-$[AlCl_3]_x$ mixture for x=0.3 did not visibly change from the appearance of a monophasic yellowish solution in the temperature range 60 °C to 90 °C when it had not been subjected to voltammetric scanning. However, if each of these large magnitude anodic current peaks is due to the dissolution of a film formed on the electrode during forward scanning in the anodic voltage range of 0 to 4 V vs Ag triflate then variations in the nature of the film might be a possible cause of these variations in peak magnitude and position.

In most of the voltammetric scans of Figures 1 to 6 covering both pure $[C_3mpip][NTf_2]$ and $[C_3mpip][NTf_2]$-$[AlCl_3]_x$ mixtures, the anodic peak in the region –0.5 to –2.75 V vs Ag triflate is followed by a cathodic wave before a sharp cathodic drop-off starts in the region –2.75 to –2.9 V vs Ag triflate as the scanning progresses in the cathodic direction. Comparing the CVs in both the $[C_3mpip][NTf_2]$ and $[C_3mpip][NTf_2]$-$[AlCl_3]_x$ mixtures, it would appear from Figures 3 to 6 that aluminium reduction occurs in the potential range –1.8 to about –3.8 V vs Ag triflate, while at cathodic potentials more negative than about –2.8 V vs Ag triflate, decomposition of the $[C_3mpip][NTf_2]$ is occurring simultaneously.

3.2. Deposition of Al and cathodic other reactions

To confirm the aluminium reduction process at –3.7 V, galvanostatic experiments were conducted in which aluminium was electrodeposited at 90 °C onto graphite and copper electrode substrates from $[C_3mpip][NTf_2]$-$[AlCl_3]_x$ (x=0.5) at potential –3.7 V for 10 min. The presence of aluminium deposits were confirmed firstly by visual inspection. Both substrates showed white metallic coatings when taken out from the cell. The deposits were then washed thoroughly with acetone and dried. Not surprisingly, given the relatively negative deposition potential of –3.7 V, the subsequent SEM-EDS analyses of the deposits showed the presence of residual ionic liquid and/or ionic liquid decomposition products on the surfaces of the electrode substrates. This was particularly evident for the graphite substrate which analysis showed the existence of isolated Al. It was found to be very hard to clean the coated graphite as the ionic liquid and/or ionic liquid decomposition products were well adhered and penetrated into the porous substrate surface.

The quality of the aluminium deposits can be seen from BSE micrographs in Figs. 7, 8, 9, 10(a) and 10(b).

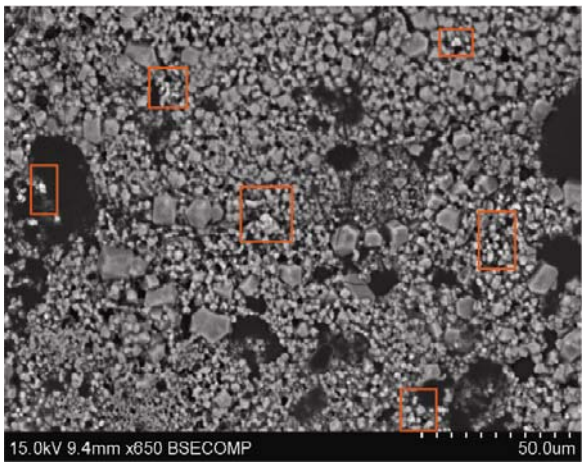

Figure 7. BSE image of aluminium electrodeposited at 90 °C from $[C_3mpip][NTf_2]$-$[AlCl_3]_x$ (x=0.5) onto graphite.

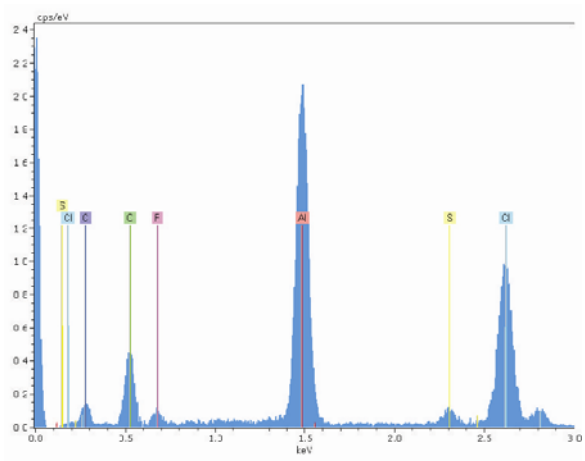

Figure 8. Energy spectra of aluminium deposits (whole area of the Figure 7 scan).

As is apparent from the highlighted regions in Figure 7 the aluminium deposits on the graphite electrode substrate appear to be in the form of crystals of up to 10 μm in size. The aluminium deposits on copper (Figures 9, 10(a) and (b)) have a fractured surface comprising large and bulky aluminium clusters with irregular shapes. The fractured clusters are thought to have been induced by mechanical stresses which occurred during the cleaning process.

From the BSE images it is evident that the nature of the electrode substrate has a great influence on the quality of the aluminium deposits.

Further Al deposition experiments were conducted with a copper electrode. There was visible Al deposition on a

copper electrode after 5 minutes at –1.0 V at 60 °C, however at higher potentials a black deposit was observed on the electrode which may have been due to the decomposition of ionic liquid leading to poisoning of the electrode surface. The products of the electrolyte decomposition may also have been passivating any aluminium deposited during the cathodic scan and preventing the appearance of the anodic re-oxidation peak on scan reversal, as would normally be expected during any metal deposition process. This might explain the absence of the expected metal re-oxidation peaks in most of the cyclic voltammograms presented above.

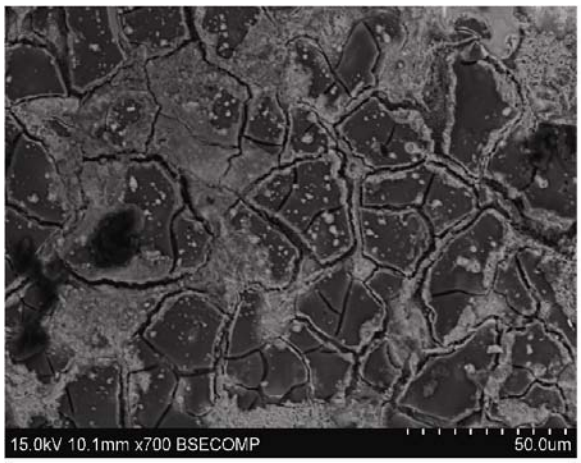

Figure 9. BSE image of Al film electrodeposited at 90 °C from $[C_3mpipNTf_2]$-$[AlCl_3]_x$ (x=0.5) onto Cu foil.

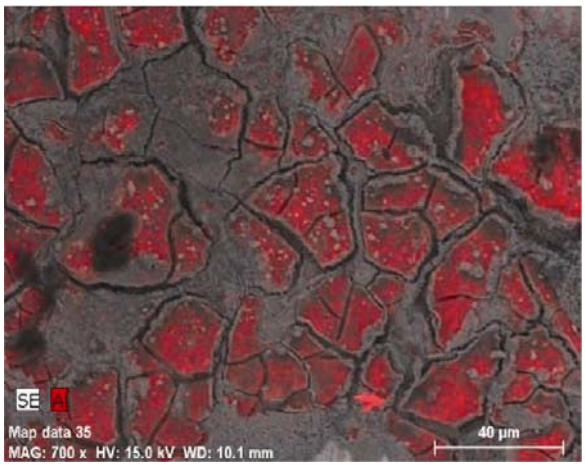

(a)

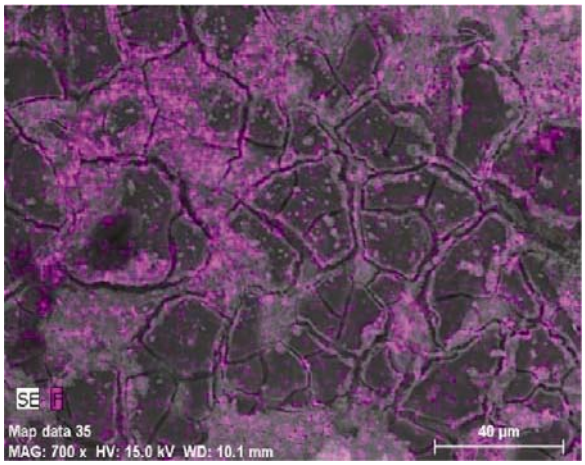

(b)

Figure 10. (a) aluminium, and (b) fluorine mapping of aluminium deposits for the image in Figure 9.

Additional cathodic potentiostatic experiments were carried out to study the deposition of Al from $[C_3mpip][NTf_2]$-$[AlCl_3]_x$ mixtures at copper electrodes as well as graphite and stainless steel electrodes. The constant potential values were chosen from previous studies and electrolysis was carried out at 90 °C for 2 hours. The chosen test potentials of –1, –1.5, –2, –2.5 and –3 V yielded no aluminium deposits however, unlike results reported previously in literature[26]. One likely reason for the failure to produce aluminium deposits in these latter experiments is thought to be at least partially due to the level of the moisture content in the ionic liquid electrolytes used in these experiments since after drying in a rotary evaporator they were not further subjected to drying in vacuo at elevated temperatures for an extended period in attempt to simulate extreme conditions that one might encounter in an industrial scenario. This view is consistent with the observations of earlier workers, albeit for a different type of ionic liquid, who have reported that even if only a small amount of water remained in the ionic liquid they were using, namely an aliphatic quaternary ammonium imide-type ionic liquid containing metal ions, even after dehydration in vacuo, it can cause some problems in metal deposition from the ionic liquid[33]. Another reason for the lack of Al deposition is probably due to the formation of a passivating film on the electrode surface caused either by the presence of a small amount of water in the ionic liquid electrolyte or by decomposition of the ionic liquid or a combination of both (see for example the BSE image of the film on the graphite electrode substrate shown in Figure 7 surrounding the isolated Al deposits). This finding suggests that if Al was to be deposited from a $[C_3mpip][NTf_2]$-$[AlCl_3]_x$ mixture on a commercial scale that the water content and the deposition potential would need to be carefully controlled for Al deposition and minimal electrolyte decomposition as was apparently done by earlier workers[26] who used thoroughly dried $[C_3mpip][NTf_2]$-$[AlCl_3]_x$ electrolytes[26] and a narrow potential range for Al deposition in order to achieve good quality deposits of Al. In addition, those earlier workers[26] indicated that $[C_3mpip][NTf_2]$ is "air- and water-stable", however, this statement should perhaps be a more qualified one that warns of the potential risks of too high a level of water in the electrolyte and of exposing the electrode on which Al is to be deposited to too negative or too positive a potential on either side of the optimum Al deposition potential range. Otherwise, a film detrimental to Al deposition may be formed on the electrode.

3.3. Anodic reactions

Linear sweep voltammograms obtained at the DSA electrode in the mixture $[C_3mpip][NTf_2]$-$[AlCl_3]_x$ (x = 0.3) are shown in Figure 11 at various temperatures and at a scan rate of 10 mV/s.

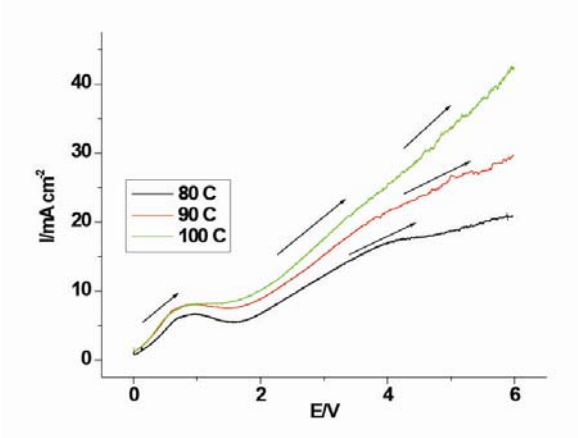

Figure 11. Linear sweep voltammograms obtained at DSA electrode for $[C_3mpip][NTf_2]$-$[AlCl_3]_x$ (x = 0.3) at various temperatures, 10 mV/s.

A small anodic peak is seen at around 1V beyond which the current increases before reaching a limiting current at about 4 V. The initial anodic peak in the 0 - 2 V range is assumed to be at least partly associated with an anodic reaction occurring prior to chlorine evolution. This peak is also present in the absence of $AlCl_3$ (see Figs. 1 and 2) and consequently it is thought to be associated with the oxidation of $[C_3mpip][NTf_2]$.

As expected, the limiting current increases with increasing temperature due to the higher diffusion rates of the reacting ions. The slope of the voltammograms is indicative of a high cell resistance. This is again expected given the low conductivity of these ionic liquids[34, 35].

Galvanostatic experiments were also carried out to confirm evolution of chlorine. After completion of the electrochemical studies the visible appearances of the mixtures changed markedly and the initial colourless appearance had changed to a light to dark yellow colour with a Cl_2 like odour. Another indication of gas formation was the presence of bubbles around the electrode. To identify the possible reaction products, further potentiostatic tests were carried out and the collected gases were analyzed using GC-MS. Scanning electron microscopy and XPS techniques were also used to investigate the nature of deposits on the electrode surfaces.

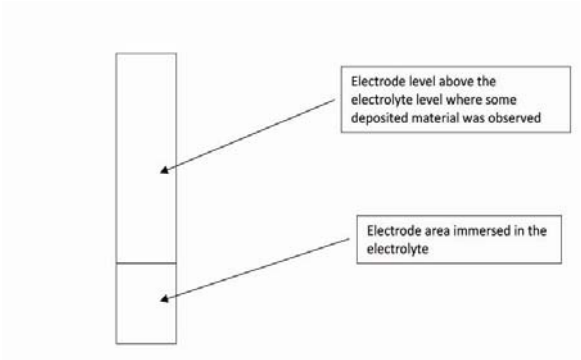

Figure 12. Schematic diagram of a DSA electrode subjected to the electrolysis tests of Figures 13 - 19.

For these studies, $[C_3mpip][NTf_2]$-$[AlCl_3]_x$ mixtures (x = 0.24, 0.35) were used as electrolytes with a DSA (Ir_2O_3 on Ti) working electrode (see Figure 12). All tests were carried out in a single compartment cell.

3.3.1. SEM and XPS analysis

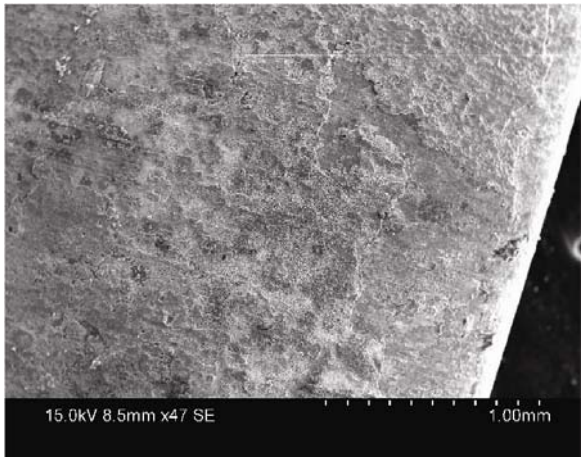

(a)

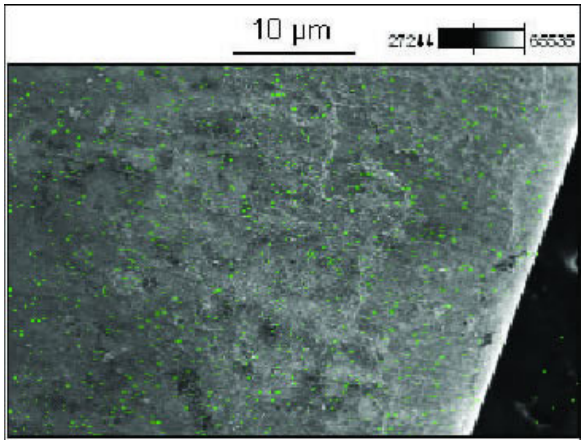

(b)(i)

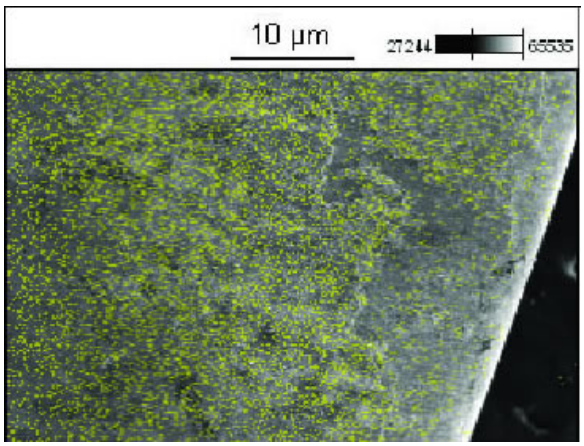

(b)(ii)

Figure 13. (a) SEM image and elemental mapping results for (b)(i) Al, and (b)(ii) Cl for a DSA anode after a potentiostatic test (2 V vs Ag/Ag triflate for 2 hours) for $[C_3mpip][NTf_2]$-$[AlCl_3]_x$ mixture (x=0.24).

Potentiostatic experiments were performed on a DSA working electrode at an anodic potential of 2 V vs Ag triflate reference electrode for 2 hours in a $[C_3mpip][NTf_2]$-$[AlCl_3]_x$ mixture (x = 0.24). The morphology of the DSA electrode was then examined for any deposits using scanning electron microscopy and elemental mapping was used to identify the deposits. Figure 13 (a) shows the SEM image of the electrode while Figures 13(b)(i) and (ii) show the corresponding mapping results for Al and Cl respectively.

The presence of aluminium and chlorine is believed to be due to physical adsorption of the ionic liquid mixture on the electrode surface as when the electrode was completely washed with acetone, these materials were not detected. To understand the exact nature of the deposits on the DSA electrode, XPS was used and binding energy value comparisons were done for better understanding of bonding involved. The corresponding XPS data are shown in Figures 14(a) and 14(b).

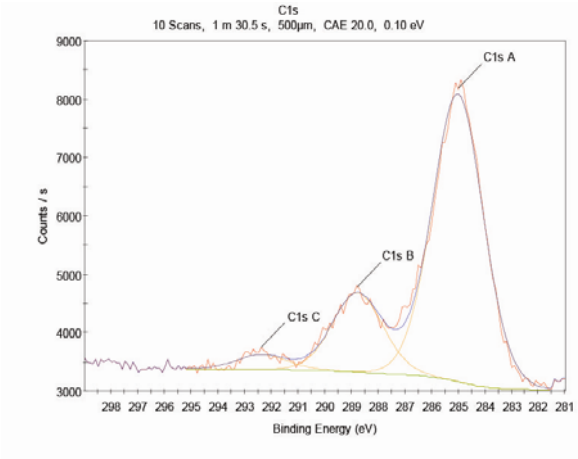

(a)

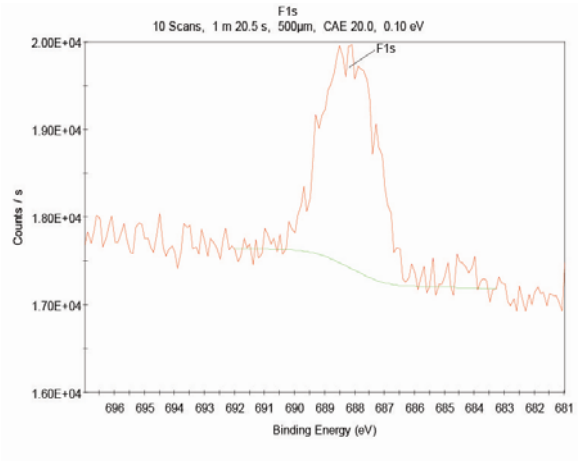

(b)

Figure 14. Binding energy spectra obtained at the DSA working electrode after a potentiostatic test in a $[C_3mpip][NTf_2]$-$[AlCl_3]_x$ mixture (x = 0.24): (a) C, and (b) F.

The spectral lines (peaks) in Figure 14(a) corresponding to binding energies 285, 289 and 291 eV values correspond to carbon (1s states) in fluorocarbon compounds[27] [e.g. CF_4, $(-CF_2-CF_2-)_n$]. This is in complete agreement with the binding energy values obtained for fluorine shown in Fig. 14(b). The peak corresponding to a binding energy of 689 is due to F(1s) state [e.g. CF_2 etc] which indicates the presence of fluorocarbons. The gas analysis for the DSA electrode is discussed later.

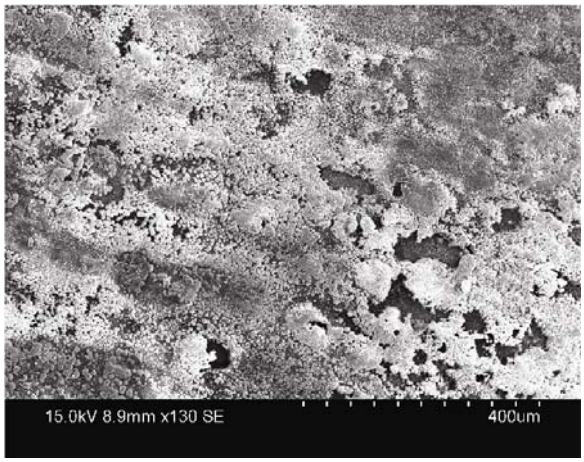

(a)

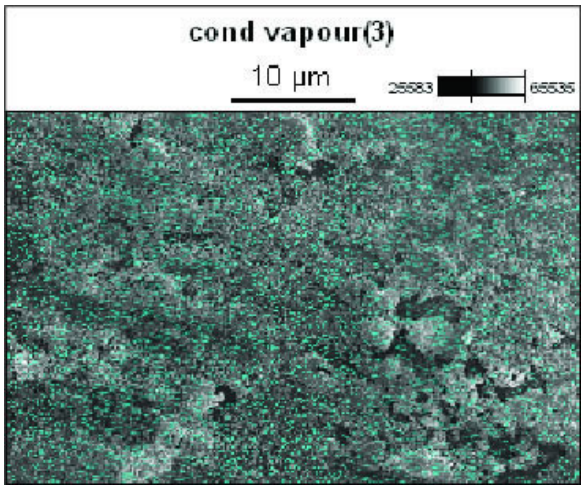

(b)(i)

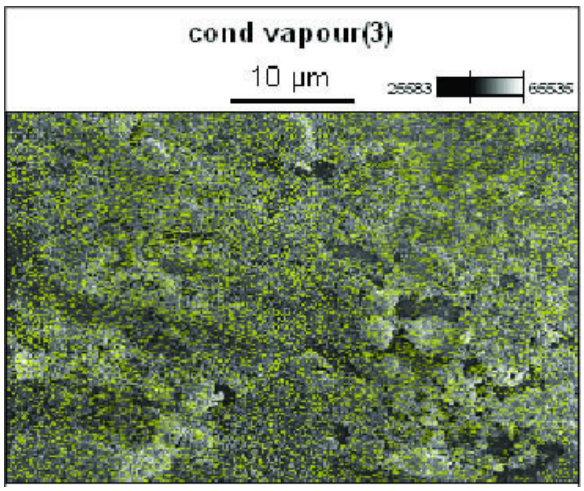

(b)(ii)

Figure 15. (a) SEM image of condensed vapours deposited on DSA electrode after a potentiostatic test (2 V for 2 hrs, 90 °C) in a $[C_3mpip][NTf_2]$-$[AlCl_3]_x$ mixture (x = 0.24) and corresponding elemental mapping for (b)(i) Al and (b)(ii) Cl.

Another interesting observation was the presence of some condensed material on the DSA working electrode that was not in contact with the electrolyte directly (see schematic in Figure 12). This deposited material was analyzed using SEM and XPS techniques. Figure 15 (a) shows the SEM image of condensed vapours on part of the electrode and Figures 15 (b)(i) and (b)(ii) show the corresponding elemental mapping for Al and Cl respectively.

These results possibly indicate the sublimation and condensation of $AlCl_3$ from the mixture. This electrode structure was also investigated using the XPS technique. XPS line spectra for the condensed vapour region using the DSA electrode are shown in Figures 16(a) and (b).

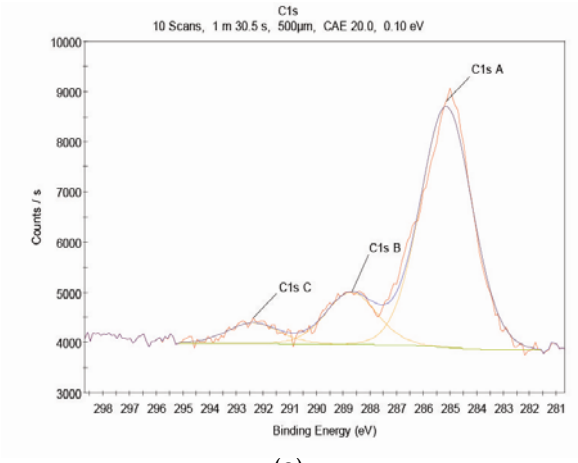

(a)

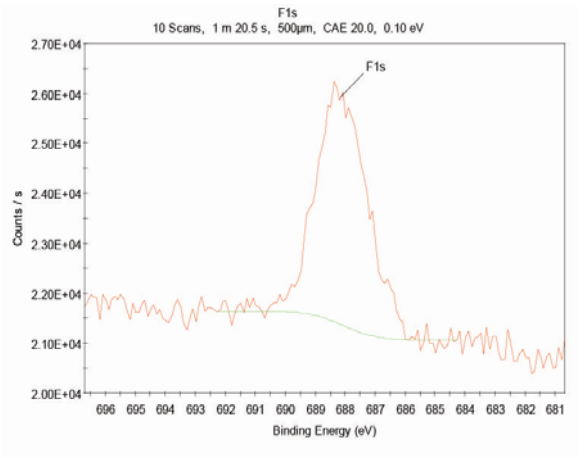

(b)

Figure 16. XPS spectra of the DSA electrode surface with deposited condensed vapours for a $[C_3mpip][NTf_2]$-$[AlCl_3]_x$ (x = 0.24) mixture at 90 °C: (a) C, and (b) F.

The peaks in Figure 16(a) corresponding to 285, 289 and 292 eV values represent C (1s spectral lines)[27]. This is characteristic for fluorocarbon compounds. Also a spectral line for F (1s spectral line) shows a peak at around 689 eV which confirms the presence of fluorocarbon based compounds $(-CF_2-CF_2-)_n$. To confirm if these compounds were actually formed as a result of an anodic reaction or decomposition of the ionic liquid due to heating (without any electrolysis), an experiment was carried out where the mixture was heated for 3-4 hrs at 90 °C and electrodes immersed in the mixture in a sealed cell. The XPS analysis of these samples confirmed the presence of fluorocarbons on the electrodes, indicating that these compounds were formed as a result of decomposition of the ionic liquid itself at higher temperatures.

3.3.2. GC-MS analysis

For identification of gaseous reaction products, mass spectral data was acquired in positive ion electron impact (EI^+) mode using a Thermo Trace DSQ II GC-MS (Thermo Scientific). Gaseous samples (100 µL) were injected onto a 30 m x 0.25 mm J&W DB5-MS capillary column (Agilent Technologies), at an initial temperature of 35 °C with helium carrier gas set to a constant flow rate of 1 mL/min. The GC temperature was ramped to 260 °C. The spectral matches were obtained using Xcalibur library associated with the instrument.

Separate experiments were carried out for a $[C_3mpip][NTf_2]$-$[AlCl_3]_x$ mixture (x = 0.35). In a first experiment the mixture was simply heated at 90 °C for 3 hours (without any electrolysis test). The GC-MS analyses qualitatively determined the presence of (a) Methanamine N,N-bis(trifluoromethoxysulfinyl); (b) Chlorotrimethyl silane; and (c) Dichloro dimethyl silane. A second mixture was subjected to electrolysis at constant potential of 3 V vs Ag triflate for 3 hrs, the gas samples were analysed using GC-MS and the analyses qualitatively determined the presence of (a) Methanamine N,N-bis(trifluoromethoxysulfinyl); (b) Ether, bis(chloro-methyl); (c) Tromethamine; (d) Chlorotrimethyl silane; and (e) Dichloro dimethyl silane. Also a fused silica column was used instead of DB5-MS capillary column and the analysis with this arrangement confirmed qualitatively that chlorine gas was being formed in the second mixture.

The GC-MS results confirm the formation of various decomposition products of the ionic liquid electrolyte even without any electrolysis tests. Cl_2 is also seen to be present since it reacts with the column to form chlorosilanes. Further, the formation of fluorocarbons found in the XPS spectra may be difficult to avoid due to the operating conditions required for Al electro-deposition. The occurrence of fluorocarbons thus suggests that on a commercial scale the process is unlikely to be environmentally friendly. Other products like trimethanamine and chloro-ethers are also formed during the electrolysis. Due to formation of these decomposition products, the ionic liquids are unlikely to be reusable in an Al deposition process. This conclusion is supported by Roudopoulos et al.[26]

3.3.3. ^{27}Al NMR spectroscopy

Aluminium speciation change during the electrolysis was investigated by ^{27}Al NMR spectroscopy using a double compartment H shaped cell. Electrolysis was conducted in a potentiostatic mode at 2.0 V vs Ag triflate at 90 °C for 20 hours in $[C_3mpip][NTf_2]$-$[AlCl_3]_x$ mixtures where x= 0.24, 0.35 and 0.45. The counter electrode was a graphite rod with a diameter of 15 mm,

the working electrode was a stainless steel wire (L= 25 mm and D= 0.8 mm) and a 0.5 mm silver wire dipped in silver triflate was used as reference electrode. The ^{27}Al NMR of electrolyte samples before the tests and samples from the cathodic and anodic compartments after tests were recorded at a temperature of 90 °C. The ^{27}Al chemical shift values were measured relative to an aqueous solution of $Al(NO_3)_3 \cdot 9H_2O$ as an external reference. The interpretation of ^{27}Al NMR spectra in connection with speciation in these mixtures is well presented by T. Rodopoulos et al.[26] and was adopted in the following analysis. The ^{27}Al NMR shifts (δ) of the resonances obtained in the experiments are shown in Figures 17 to 19.

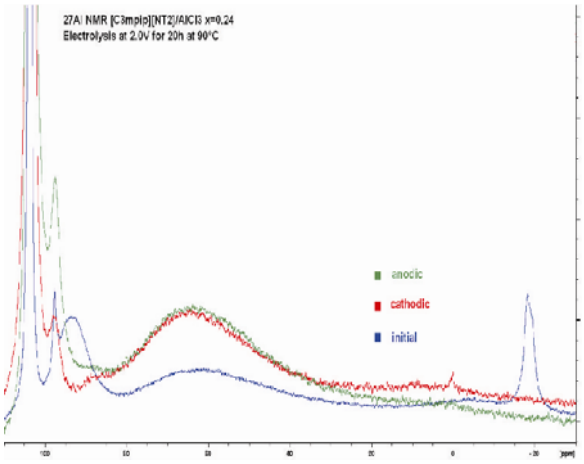

Figure 17. The ^{27}Al NMR spectra of $[C_3mpip][NTf_2]$-$[AlCl_3]_x$ mixture at x=0.24 taken at 90 °C before and after electrolysis test. Cell voltage kept 2.0 V for 20 h at 90 °C.

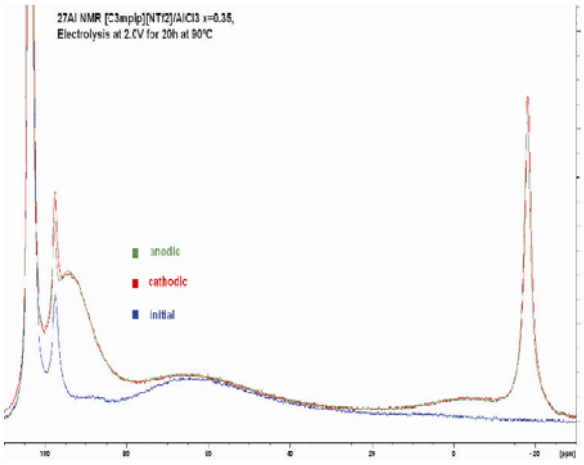

Figure 18. The ^{27}Al NMR spectra of $[C_3mpip][NTf_2]$-$[AlCl_3]_x$ mixture at x=0.35 taken at 90 °C before and after electrolysis test. Cell voltage kept 2.0 V for 20 h at 90 °C.

The ^{27}Al NMR shifts (δ) of the resonances obtained in the experiments are summarized in Table 2. All samples showed the dominant strong resonance at δ=104 ppm (Figs. 17-19) which has been assigned previously to the presence of a 4-coordinated $AlCl_4^-$ ion[26]. The following equilibrium has been suggested in $[C_3mpip][NTf_2]$-$[AlCl_3]_x$ mixtures:

$$2NTf_2^- + 2AlCl_3 \leftrightarrow AlCl_4^- + AlCl_2(NTf_2)_2^- \quad K_1 \quad (2)$$

A large equilibrium constant K_1 for reaction (2) would account for the strong resonance observed.

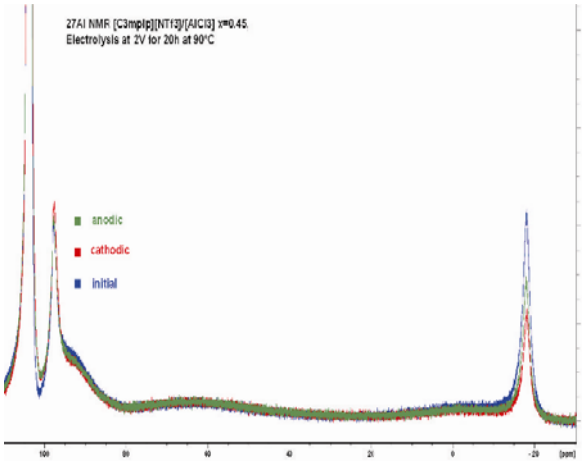

Figure 19. The ^{27}Al NMR spectra of $[C_3mpip][NTf_2]$-$[AlCl_3]_x$ mixture at x=0.45 taken at 90 °C before and after electrolysis test. Cell voltage kept 2.0 V for 20 h at 90 °C.

Table 2. ^{27}Al NMR shifts (δ) of the resonances in the spectra of $[C_3mpip][NTf_2]$-$[AlCl_3]_x$ mixtures for x= 0.24, 0.35 and 0.45 initially and mixtures in the anodic and cathodic chambers after being held at 2 V at 90 °C for 20 h.

x	Sample	δ [ppm] for $[C_3mpip][NTf_2]$-$[AlCl_3]_x$
0.24	Initial mixture	104 s, 98m, 94m, –5vw, –18m
	Anodic chamber mixture	104 s, 98m
	Cathodic chamber mixture	104 s, 98m, –1w
0.35	Initial mixture	104 s, 98m, 90w
	Anodic chamber mixture	104 s, 98m, 94m, –3vw, –18m
	Cathodic chamber mixture	104 s, 98m, 94m, –3vw, –18m
0.45	Initial mixture	104 s, 98m, 94mw, –3vw, –18m
	Anodic chamber mixture	104 s, 98m, 94mw, –3vw, –18m
	Cathodic chamber mixture	104 s, 98m, 94mw, –3vw, –18m

A peak similar to the medium resonance at δ=98 ppm found in all test samples has been assigned in previous studies to being due to a hydrolysis product[26,36]. Analogously, we suggest the medium resonance at δ=98 ppm found in the present study is likely to be due to a hydrolysis product resulting from the reaction of residual water with the $[C_3mpip][NTf_2]$-$[AlCl_3]_x$ mixtures. Franzen et al.[37] identified hydrolysis products as Al_2Cl_6OH and Al_2OCl_5 using secondary ion mass spectrometry. Other reaction products were determined by passing nitrogen gas over a $[C_3mpip][NTf_2]$-$[AlCl_3]_x$ mixture and bubbling the off-gas in a silver nitrate solution for 2 hours. The silver nitrate solution showed a transparent to milky appearance transition which is indicative of the presence of chlorine ions (Cl^-). The absence of aluminium ions in the silver nitrate solution

was verified by an alizarin test. These tests suggest that another by-product was hydrogen chloride (HCl). The magnitude of the peak at δ=98 ppm is consistent with the electrolytes containing more hydrolysis products than has been reported in an earlier study[26] in which the magnitude of the peak at δ=98 ppm was weak. This would at least partly explain the poor Al deposition outcomes obtained in the present study compared with those reported earlier[26], but once again casts doubt on the industrial viability of these apparently moisture sensitive ionic liquids.

The tetrahedral $[AlCl_3\text{-}(NTf_2)]^-$ electro-active ion resonance at δ=94 ppm (assigned previously by T. Rodopoulos et al.[26] and thought to be the 4-coordinate Al species from which Al can be electrodeposited) is evident in the initial mixtures with x= 0.24 and 0.45 (Figs. 13 and 15) and is not present in the initial mixture with x=0.35 (Fig. 14) although both cathodic and anodic samples with x=0.35 showed the resonance at δ=94 ppm in the form of a broad shoulder adjacent to a hydrolysis resonance at δ=98 ppm. The aluminium electro-active ion resonance at δ=94 ppm correlates with the presence of an octahedral $Al(NTf_2)_3$ complex at δ=–18 ppm (see Figs. 17-19) (assigned previously by T. Rodopoulos et al.[26] and thought to be due to a number of isomers of $Al(NTf_2)_3$). In addition to this, it can be noted that cathodic and anodic x=0.24 sample mixtures showed neither δ=94 nor δ=–18 ppm resonances at a given temperature. These correlations suggest that both the $Al(NTf_2)_3$ complex and the $[AlCl_3\text{-}(NTf_2)]^-$ electro-active ion could be the equilibrium products of some reaction. These results support the following equilibrium reaction:

$$2AlCl_2(NTf_2)_2^- \leftrightarrow AlCl_3(NTf_2)^- + Al(NTf_2)_3 + Cl^- \quad K_2 \quad (3)$$

It should be noted that this correlation is only valid at temperatures above 55 °C. At temperatures below 55 °C the electro-active ion $[AlCl_3\text{-}(NTf_2)]^-$ becomes unstable, while the $Al(NTf_2)_3$ complex is well manifested in ^{27}Al NMR spectrum[26].

The lack of an $Al(NTf_2)_3$ complex resonance in the initial sample mixture with x=0.35 could be due to slow kinetics of reaction (2) during $AlCl_3$ dissolution although this would need to be confirmed by further experiments.

The presence of the octahedral ion $AlCl_2(NTf_2)_2^-$ resonance at δ=–3 ppm is clearly visible in the cathodic sample spectrum with x=0.24 (Fig. 17) and both the cathodic and anodic samples' spectra with x=0.35 (Fig. 18). It also has a faint presence in all samples with x=0.45 (Fig. 19). The low intensity for this resonance is likely to be due to a very high equilibrium constant K_2 for reaction (3) that provides a very low relative concentration of the $AlCl_2(NTf_2)_2^-$ ion in $[C_3mpip][NTf_2]\text{-}[AlCl_3]_x$ mixtures.

The broad resonance at around δ=66 ppm in all spectra is due to aluminium in the solid material used in the probe and is not associated with the sample mixtures. This is consistent with the electrode reactions being:

Cathode:

$$[AlCl_3\text{-}(NTf_2)]^- + 3e^- = Al + 3Cl^- + (NTf_2)^- \quad (4)$$

Anode:

$$2Cl^- - 2e^- = Cl_2(g) \quad (5)$$

although the chlorine ion is very likely to be part of an aluminium complex ion coordination, so the anode reaction is more likely to be of the form:

Anode:

$$2AlCl_4^- - 2e^- = 2AlCl_3 + Cl_2(g) \quad (6)$$

The tetrahedral $AlCl_4^-$ (δ=104) resonance decreased in intensity for anodic samples with x = 0.24 and 0.45. The $AlCl_3$ product is expected to be consumed by reaction (1) and partially sublimes as was noted earlier with DSA anodes.

No aluminium was deposited on the graphite rod cathode during the tests suggesting that another cathodic reaction is occurring at the set potential that would explain a decrease in resonance intensities for both tetrahedral $AlCl_4^-$ and octahedral $Al(NTf_2)_3$ ions and the presence of $AlCl_2(NTf_2)_2^-$ resonance in the cathodic samples, namely:

Cathode:

$$Al(NTf_2)_3 + 2AlCl_4^- + e^- = AlCl_2(NTf_2)_2^- + 2AlCl_3 + (NTf_2)^- \quad (7)$$

Alternatively, a plausible reason for the absences of aluminium deposits is the hydrolysis of the electro-active ion $[AlCl_3\text{-}(NTf_2)]^-$ and possible electrode passivation. A more rigorous drying procedure both in preparation and testing of these liquids should prevent deactivation of the $[C_3mpip][NTf_2]\text{-}[AlCl_3]_x$ mixtures, but this would be a significant additional cost on an industrial scale.

4. Conclusion

In the present study of the deposition of aluminium and other cathodic reactions, the ionic liquid was not stable since decomposition products co-deposited on the electrode at the Al deposition potential investigated of –3.7 V. In addition, the deposition of aluminium from $[C_3mpip][NTf_2]\text{-}[AlCl_3]_x$ mixtures was generally found to be highly inconsistent and it is thought that sensitivity of the ionic liquid mixtures to moisture and exposure of the electrode substrate to a deposition voltage in which decomposition of the ionic liquid is occurring simultaneously is at least partly responsible for the presence of passivation products on the electrode surface during deposition.

In the present study of the anodic reactions taking place in $[C_3mpip][NTf_2]\text{-}[AlCl_3]_x$ mixtures using glassy carbon electrodes and dimensionally stable anodes (DSA) (Ir_2O_3 on Ti) at various compositions and temperatures indicated that some decomposition of the ionic liquid was occurring at least under the conditions investigated. Formation of Cl_2 was confirmed to take place at dimensionally stable anodes as a part of the anodic reaction of $[C_3mpip][NTf_2]\text{-}[AlCl_3]_x$ mixtures (at least when x=0.35); however analysis of the mixture indicated that at temperatures near to a potential operating temperature of the $[C_3mpip][NTf_2]\text{-}[AlCl_3]_x$ the mixture at least partially decomposes into fluoro-carbons (at least when x=0.24) and other chloro-compounds (at least when x=0.35). It would appear therefore, that the formation of fluorocarbons, at least for the ionic liquids investigated in this study, may be difficult to avoid under the operating

temperature required for Al electro-deposition from a $[C_3mpip][NTf_2]$-$[AlCl_3]_x$ mixture. The formation of these anodic decomposition products has the further disadvantage that the $[C_3mpip][NTf_2]$ liquid may be difficult to reuse.

In summary, the ionic liquids may have a poor usage life and may need to be regularly replaced under industrial operation due to the potential anodic reactions as illustrated in the present study by the decomposition reactions found to be occurring at a DSA electrode at a potential of around 2 V vs Ag triflate under typical conditions envisaged for aluminium deposition. Given this and the apparent additional disadvantages of moisture sensitivity of Al electro-deposition in these ionic liquids, the inconsistency of Al deposition and the potential for the cathodic decomposition of the ionic liquid and the co-deposition of the resultant electrolyte decomposition products on the cathode as has been shown to occur when the potential of the cathode is made too negative, a commercial process of electro-deposition of Al from $[C_3mpip][NTf_2]$-$[AlCl_3]_x$ mixtures may prove to be difficult to develop and perform satisfactorily on an industrial scale.

5. Acknowledgement

This work was conducted as part of a research cluster entitled "Breakthrough technologies for primary aluminium" established between five Australian universities and the CSIRO Light Metals Flagship and was funded by the CSIRO National Research Flagships Collaboration Fund.

6. References

[1] Hall C. M., *US 400664*, **1889**.

[2] Welch B. J., *J. of Minerals, Metals and Materials Society*, **1999,** *51*, 24.

[3] Gielen D. J., *Methodological Aspects of Resource-Oriented Analysis of material Flows, Workshop. The Future of the European Aluminium Industry: A MARKAL Energy and Material Flow Analysis*, **1998**.

[4] Zhang M., Kamavaram V., Reddy R.G., *J. Organomet. Chem.*, **2003**, *11*, 54.

[5] Kamavaram V., Mantha D., Reddy R.G., *Electrochim. Acta*, **2005,** *50*, 3286.

[6] Kamavaram V., Mantha D., Reddy R.G., *J. Min Metall.*, **2003,** *B39(1-2)*, 43.

[7] Reddy R.G., *J. of Physics: Conference Series*, **2005,** *165*, 012076.

[8] Lehmkuhl H., Mehler K., Landau U., in: *Gerischer H., Tobias C.W., (Eds.), Advances in Electrochemical Science and Engineering, Vol. 3, VCH Verlagsgesellschaft, Weinheim*, **1990,** 165.

[9] Zhao Y., VanderNoot T. J., *Electrochim. Acta*, **1997,** *42*, 1639.

[10] Liao Q., Pitner W. R., Stewart G., Hussey C. L., Stafford G. R., *J. Electrochem. Soc.*, **1997,** *144*, 936.

[11] Zell C. A., Endres F., Freyland W., *Phys. Chem. Chem. Phys.*, **1999,** *1*, 697.

[12] Endres F., Bukowski M., Hempelmann R., Natter H., *Angew. Chem.*, **2003,** *115*, 3550; *Angew. Chem. Int. Ed.*, **2003,** *42*, 3428.

[13] Lu J., Dreisinger D., in *Ionic Liquids as Green Solvents: Progress and Prospects (Eds.: R. D. Rogers, K. R. Seddon), American Chemical Society,* Washington, DC, **2003,** 495.

[14] Abbott P., Eardley C. A., Farley N. R. S., Griffith G. A., Pratt A., *J. Appl. Electrochem.*, **2001,** *31*, 1345.

[15] Kamavaram V., Reddy R. G., *Metal Separation Technologies III, Engineering Conferences International*, Brooklyn, NY, **2004,** 143.

[16] Jiang T., Chollier Brym M. J., Dub G., Lasia A., Brisard G. M., *Surf. Coat. Technol.*, **2006,** *201*, 1.

[17] Welch B. J., Osteryoung R. A., *J. Electroanal. Chem.*, **1981,** *118*, 455.

[18] Chum H. L., Osteryoung R. A., in *Ionic Liquids (Eds: Inman D., Lovering D. G.)*, *Plenum Press*, New York, **1981,** 407.

[19] Auborn J. J., Barberio Y. L., *J. Electrochem. Soc.*, **1985,** *132*, 598.

[20] Jones S. D., Blomgren G. E., *J. Electrochem. Soc.*, **1989,** *136*, 424.

[21] Carlin R. T., Crawford W., Bersch M., *J. Electrochem. Soc.*, **1992,** *139*, 2720.

[22] Jiang T., Chollier Brym M. J., Dube G., Lasia A., Brisard G. M., *Surf. Coat. Technol.*, **2006,** *201*, 10.

[23] Gao L., Wang L., Li Y., Chu J., Qu J., *Acta Phys. Chim. Sin.*, **2008,** *24*, 939.

[24] Robinson J., Osteryoung R. A., *J. Electrochem. Soc.*, **1980,** *127*, 122.

[25] Rocher N. M., Izgorodina E. I., Ruther T., Forsyth M., MacFarlane D. R., Rodopoulos T., Horne M. D., Bond A. M., *Chem. Eur. J.*, **2009,** *15*, 3435.

[26] Rodopoulos T., Smith L., Horne M. D., Ruther T., *Chem. Eur. J.*, **2010,** *16(12)*, 3815.

[27] Zein El Abedin S., Moustafa E. M., Hempelmann R., Natter H., Endres F., *Electrochemistry Communications*, **2005,** *7(11)*, 1111.

[28] Horne M. D., Rodopoulos T., Smith L., Ruether T., *Proceedings of 2nd International Congress on Ionic Liquids (COIL-2)*, Yokohama, Japan, August 5th - 10th, **2007,** 3P07-076, 385.

[29] Zein El Abedin S., Moustafa E. M., Hempelmann R., Natter H., Endres F., *Chem. Phys. Chem.*, **2006,** *7*, 1535.

[30] Carlin R. T., Osteryoung R. A., *J. Electrochem. Soc.*, **1989,** *136*, 1409.

[31] Lai P. K., Skyllas-Kazacos M., *J. Electroanal. Chem.*, **1988,** *248*, 431.

[32] Rocher N. M., Clare R., Izgorodina E. I., Bond A., Forsyth M., MacFarlane D., Horne M., Rodopoulos T., *Proceedings of 2nd International Congress on Ionic Liquids (COIL-2)*, Yokohama, Japan, August 5th - 10th, **2007,** 243.

[33] Katase T., Imashuku S., Murase K., Hirato T., Awakura Y., *Science and Technology of Advanced Minerals*, **2006,** *7*, 502.

[34] Endres F., Zein El Abedin S., *Phys. Chem. Chem. Phys.*, **2006,** *8*, 2101.

[35] Zhang M., Kamavaram V., Reddy R. G., *Minerals and Metallurgical Processing*, **2006,** *23(4)*, 177.

[36] Takahashi S., Saboungi M. L., Klinger R. J., Chen M. J., Rathke J. W., J. *Chem. Soc. Faraday Trans.*, **1993,** *89*, 3591.

[37] Franzen G., Gilbert B. P., Pelzer G., DePauw E., *Org. Mass. Spectrom.*, **1986,** *21*, 443.

Received: 31.10.2012.
Accepted: 09.11.2012.